# Quantitative and functional posttranslational modification proteomics reveals that TREPH1 plays a role in plant touch-delayed bolting

Kai Wang[a,b,c,1], Zhu Yang[a,b,c,d,1], Dongjin Qing[a,b,c,1], Feng Ren[a,b,c,1], Shichang Liu[a,b,c], Qingsong Zheng[a,b,c,e], Jun Liu[f], Weiping Zhang[f], Chen Dai[e], Madeline Wu[a,b,c], E. Wassim Chehab[g], Janet Braam[g], and Ning Li[a,b,c,d,2]

[a]Division of Life Science, The Hong Kong University of Science and Technology, Hong Kong SAR, China; [b]Energy Institute, The Hong Kong University of Science and Technology, Hong Kong SAR, China; [c]Institute for the Environment, The Hong Kong University of Science and Technology, Hong Kong SAR, China; [d]HKUST Shenzhen Research Institute, 518057 Shenzhen, China; [e]Proteomics Center, College of Resources and Environmental Sciences, Nanjing Agricultural University, 210095 Nanjing, China; [f]ASPEC Technologies Limited, 100101 Beijing, China; and [g]Department of BioSciences, Rice University, Houston, TX 77005

Edited by Krishna K. Niyogi, Howard Hughes Medical Institute and University of California, Berkeley, CA, and approved September 7, 2018 (received for review August 21, 2018)

**Environmental mechanical forces, such as wind and touch, trigger gene-expression regulation and developmental changes, called "thigmomorphogenesis," in plants, demonstrating the ability of plants to perceive such stimuli. In *Arabidopsis*, a major thigmomorphogenetic response is delayed bolting, i.e., emergence of the flowering stem. The signaling components responsible for mechanotransduction of the touch response are largely unknown. Here, we performed a high-throughput SILIA (stable isotope labeling in *Arabidopsis*)-based quantitative phosphoproteomics analysis to profile changes in protein phosphorylation resulting from 40 seconds of force stimulation in *Arabidopsis thaliana*. Of the 24 touch-responsive phosphopeptides identified, many were derived from kinases, phosphatases, cytoskeleton proteins, membrane proteins, and ion transporters. In addition, the previously uncharacterized protein TOUCH-REGULATED PHOSPHOPROTEIN1 (TREPH1) became rapidly phosphorylated in touch-stimulated plants, as confirmed by immunoblots. TREPH1 fractionates as a soluble protein and is shown to be required for the touch-induced delay of bolting and gene-expression changes. Furthermore, a nonphosphorylatable site-specific isoform of TREPH1 (S625A) failed to restore touch-induced flowering delay of *treph1-1*, indicating the necessity of S625 for TREPH1 function and providing evidence consistent with the possible functional relevance of the touch-regulated TREPH1 phosphorylation. Taken together, these findings identify a phosphoprotein player in *Arabidopsis* thigmomorphogenesis regulation and provide evidence that TREPH1 and its touch-induced phosphorylation may play a role in touch-induced bolting delay, a major component of thigmomorphogenesis.**

thigmomorphogenesis | force-induced phosphoproteome | 4C PTM proteomics | touch-regulated phosphoprotein | TREPH1

Plants perceive and respond to mechanical forces, including those resulting from extracellular stimuli such as wind and rain, as well as stimuli manifested during cell proliferation and the differential growth of neighboring cells (1–7). Plants respond to mechanostimulation throughout growth and development (2, 8), and these responses are thought to play essential roles in pattern formation (9). Mechanical signals derived from cellular activities are integrated with the gravitational forces that are constantly imposed on plants through the weight of cellular components such as amyloplasts and the central vacuole (10, 11). Responses to gravitational forces include tropisms, whereby shoots grow away from the gravitational pull of the earth and roots grow toward this force (12). Reaction wood in conifer trees and many flowering plants is produced when woody stem tissues expand differentially due to the gravitational force imposed by the weight of the stem (13). Some plants display thigmotropic ("thigmo" means "touch" in Greek) growth, whereby a touch stimulus results in growth directed toward or away from the stimulus contact point; an exemplary thigmotropic response is the directed coiling of a climbing plant tendril around a supporting object (14). Touch-induced plant movements that occur in a direction independent of the stimulus direction are called thigmonastic responses (15) and include the dramatic rapid touch-induced leaf movements of *Mimosa pudica* and the carnivorous Venus flytrap plant (16). Thigmomorphogenesis is a slower touch response that affects overall plant growth (17). Thigmomorphogenesis can be quite dramatic and is widespread among plants. Thigmomorphogenesis can result from diverse environmental factors, such as wind, rainfall, hail, animal contact, and even the touch of a plant organ itself (13, 18). Frequent touch stimulation of *Arabidopsis thaliana* leaves triggers delayed

## Significance

Plants respond to a delicate force signal, such as a light touch, similar to animal neural systems, as demonstrated by thigmotropism, thigmonastic movement, and thigmomorphogenesis. To understand the force-signaling networks, we applied stable isotope labeling in *Arabidopsis* (SILIA)-based quantitative posttranslational modification proteomics to assess protein phosphorylation changes in *Arabidopsis* subjected to 40-second cotton-swab touch, identified 4,895 nonredundant phosphopeptides, 579 of which are previously unreported phosphosites derived from 509 phosphoprotein groups, and identified 24 TOUCH-REGULATED PHOSPHOPROTEIN (TREPH) groups. Molecular biological, genetic, and bioinformatic analyses revealed that the previously uncharacterized TREPH1 protein is required for the bolting-delay aspect of the *Arabidopsis* touch response. These studies suggest that protein phosphorylation and the TREPH1 protein are critical for the mechanotransduction pathway leading to an aspect of plant thigmomorphogenesis.

Author contributions: N.L. designed research; K.W., Z.Y., D.Q., F.R., S.L., Q.Z., J.L., W.Z., C.D., and E.W.C. performed research; Z.Y. and N.L. contributed new reagents/analytic tools; J.L., W.Z., and C.D. performed preliminary MS/MS analysis; E.W.C. and J.B. constructed transgenic LUC plants; K.W., Z.Y., D.Q., F.R., S.L., Q.Z., and N.L. analyzed data; and K.W., Z.Y., M.W., J.B., and N.L. wrote the paper.

The authors declare no conflict of interest.

This article is a PNAS Direct Submission.



Data deposition: The proteomic data reported in this paper have been deposited in the ProteomeXchange database (accession nos. PXD006180 and PXD006181).

[1]K.W., Z.Y., D.Q., and F.R. contributed equally to this work.

[2]To whom correspondence should be addressed. Email: boningli@ust.hk.

This article contains supporting information online at www.pnas.org/lookup/suppl/doi:10.1073/pnas.1814006115/-/DCSupplemental.

Published online October 5, 2018.

PLANT BIOLOGY

flowering (2, 19), and long-term wind-entrained trees can become stocky (20).

Specialized mechanosensory cells or structural appendages of plants may participate in sophisticated mechanoresponses. For example, specialized endodermal and columella cells can sense changes in orientation relative to the gravity vector (21–24). The modified leaves in the Venus flytrap and mimosa petioles harbor trigger-hair gland cells and pulvinar cells, respectively, which perceive touch signals (2). Root tips are also highly responsive to mechanostimulation; upon encountering growth barriers, specialized mechanosensing founder cells initiate a barrier-avoidance response that can promote lateral root initiation (25).

How plants sense various mechanical stimuli and transduce signals to regulate their diverse responses to touch signals remains elusive (2, 9). One class of potential plant mechanoreceptors has been identified based on studies of homologs of well-characterized mechanosensitive ion channels from microbes and animals (26–28). For example, plant mechanosensitive channel of small conductance (MscS)-like (MSL) ion channels, mating-induced death1 (MID1)-complementing activity (MCA) calcium channels, and two-pore potassium (TPK) channels are homologs of those in bacteria, yeasts, and animals, respectively (29, 30). Recently, *Piezo*, a mechanosensitive ion channel identified in humans, was found to have plant homologs that may function as selective calcium ion channels that are responsive to a wide array of force stimuli (31, 32). Examples of these homologs include MSL8, which functions in pollen hydration and seed germination (8), and MCA1/2 proteins, which are stretch activated and function as mechanosensitive cation channels in *Arabidopsis* and promote calcium fluctuations upon mechanical loading. Another class of potential mechanoreceptors consists of multimeric protein complexes that span the plasma membrane (30); these include the epithelial $Na^+$ channel (ENaC) protein complex of the sodium channel superfamily and the MEC/DEG channels (33). A subtype of these tethered mechanosensitive channel complexes is the transient receptor potential (TRP) cation channels, a superfamily that includes numerous non–voltage-gated $Ca^{2+}$ channels such as TRPN (34). A third class of multiprotein mechanosensors includes cadherins and integrins, which span the plasma membrane and physically interconnect the intracellular actomyosin cytoskeleton with extracellular matrix (ECM) fibronectin proteins (6). This group of multiprotein mechanosensors is usually associated with RhoA/Rho-associated coiled-coil–containing kinase (ROCK), focal adhesion kinase (FAK), Scr tyrosine kinase, and Rho/Ras kinases, which function as mechanosensitive motors that phosphorylate downstream protein substrates upon mechanical force loading (6, 35). These proteins convert force signals into diverse downstream ion currents and biochemical signals and induce protein–protein interactions, leading to touch-inducible gene expression and mechanoresponses.

Due to the potential functional redundancy and heteromeric nature of these force receptors, forward genetic screening for components of the mechanosensory and mechanoresponse machinery may not be sufficient for identifying their functions (3, 9). To circumvent this problem, we used the high-throughput stable isotope labeling in *Arabidopsis* (SILIA)-based (36) quantitative posttranslational modification (PTM) proteomic approach to identify potential force signaling components that may be important for *Arabidopsis* thigmomorphogenesis. Consistent with this possibility, proposed mechanosensitive sensors harbor kinase activity (37–40), and touch-induced gene expression is sensitive to chemical modulators of protein phosphorylation (41). Thus, we focused our study on profiling touch-induced and rapidly phosphorylated sites of plant proteins to identify potential force-signaling components involved in regulating *Arabidopsis* thigmomorphogenesis. We successfully identified 24 touch-responsive phosphopeptides. To conduct an in-depth investigation of the touch-response relevance of these candidates, we chose to focus on a candidate phosphoprotein, TOUCH-REGULATED PHOSPHOPROTEIN1 (TREPH1). Our findings indicate that TREPH1 is required for touch-induced bolting delay and point to a critical requirement for the amino acid serine 625 of TREPH1, which is phosphorylated upon plant touch stimulation. Taken together, our findings demonstrate that protein phosphorylation dynamics plays an important role in force signaling in *Arabidopsis*.

## Results

**A Light Touch Treatment Reproducibly Triggers a Cytosolic Calcium Increase, Gene-Expression Changes, and Delayed Bolting in *Arabidopsis*.** In *Arabidopsis*, touch treatment leads to a delay in the emergence of the flowering inflorescence stem, a process called "bolting," in addition to reducing the average rosette radius and inflorescence stem height (2, 19), and this response is associated with signal-specific calcium signatures (42). To elucidate the dosage effect of touch on morphogenesis, we treated five groups of *Arabidopsis* plants with one touch per second for 10–80 s (Fig. 1*A*). A repetitive touch treatment of 10-s duration (10 consecutive touches in each round of touch treatment, 1 s per touch) for three rounds daily was sufficient to trigger a significant bolting delay (Fig. 1*A*). The touch response increased with increasing duration of each round of treatment, reaching the maximum at 40-s touch treatment per round. We confirmed the cellular effect of a 40-s treatment in both Pro35S::Aequorin (AEQ) (42) and ProCML39::LUC/Col-0 (LUC) transgenic plants. The 40-s touch treatment triggered a rise in luminescence reporting rapid elevation of the cytoplasmic calcium concentration, $[Ca^{2+}]_{cyt}$, in the AEQ plants and a rise in luminescence reflecting increased expression of the recombinant gene ProCML39::LUC (Fig. 1*B* and *SI Appendix*, Fig. S1), consistent with evidence for CML39 touch inducibility of expression (43). The experimentally measured force of the cotton-swab treatment (Movies S1 and S2) was 84 ± 80 mg per touch (Fig. 1*C*). Thus, the force applied to the plants was 0.84 ± 0.8 mN per touch (gravity constant $g$ = 10 m/s$^2$), which was close to our targeted 1 mN (*SI Appendix*, *Supplementary Materials and Methods*). The repetitive 40-s touch (one touch/s) treatment at that force resulted in delayed bolting in *Arabidopsis* plants (Fig. 1*D* and *SI Appendix*, Fig. S2). In addition to the treatment using cotton swabs, touch treatments with similar force, repetitions, and frequency (the number of rounds/d) were also performed with soil-grown plants using touch administered by a gloved finger and touch administered by an automated machine that brushed human hair across the leaf surfaces (Movie S3). These diverse treatments similarly delayed bolting (*SI Appendix*, Figs. S3–S5).

**Quantitative Phosphoproteomic Analysis of Early Mechanotransduction Signaling Components During Thigmomorphogenesis.** We analyzed the 40-s–touched *LUC* plants using the SILIA-based quantitative phosphoproteomic approach (*SI Appendix*, Fig. S6) (44) to identify the phosphoproteins present during early touch-response signaling. Our 4C quantitative PTM proteomics (44) integrates (*i*) chemical labeling, (*ii*) chromatographic separation and enrichment of PTM proteins and peptides followed by mass spectrometry analysis, with (*iii*) computational analysis of PTM peptides using software for identification, quantitation, and statistical evaluation, followed by (*iv*) confirmation using biochemical and/or functional analysis. To achieve this objective, we first selected *LUC* plants for PTM proteomics analysis, as these plants report dynamic touch responses (Fig. 1*B* and *SI Appendix*, Fig. S1). We employed $^{14}N$- and $^{15}N$-labeled plants as either the control or touch-treated plant samples in both forward and reciprocal mixing experiments (Fig. 2). Six biological replicates (*SI Appendix*, *Supplementary Materials and Methods*) were

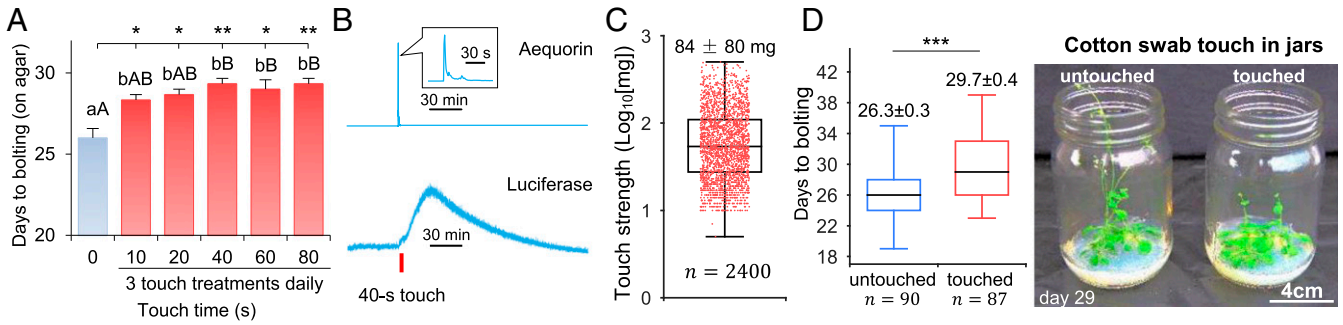


**Fig. 1.** The effect of touch on *Arabidopsis*. (*A*) The dose-dependent effect of touch using cotton swabs on bolting time. Twelve-day-old *LUC* transgenic plants were subjected to three rounds of touch treatment per day. Each round consisted of 0, 10, 20, 40, 60, or 80 touches (1 s per touch). Data are shown as means ± SE. Statistical analysis was performed using a pairwise Student's *t* test: $*P < 0.05$ and $**P < 0.01$. The homogeneity of variance among the results was analyzed using Tukey's range test. Different lowercase and uppercase letters represent significant differences at the 5% and 0.5% level, respectively. The results were compiled from three independent biological replicates, with $n \geq 27$ plants per replicate. (*B*) Photonic reporting of calcium flux and luciferase expression in transgenic *Arabidopsis* after 40 s of cotton-swab touch. Ten-day-old *AEQ* and 14-d-old *LUC* transgenic plants were subjected to 40 s of touch treatment (1 s per touch). Luminescence levels of aequorin and luciferase peaked within 60 s and at 30 min, respectively. The *Inset* shows the luminescence peaked from −0.5 to 1.5 min. The results of other two replications are shown in *SI Appendix*, Fig. S1. (*C*) Box-and-whisker plot of touch force using cotton swabs. The data points that were collected from $n = 2{,}400$ touches on 30 wild-type and 30 *treph1-1* plants (40 touches per plant) are scattered over the box-and-whisker plot. Means ± SE are annotated above the plot, defined as the typical touch force or "gentle touch." The touch force median was 54 mg, the upper quartile was 110 mg, and the lower quartile was 28 mg. The maximum was 232 mg, and the minimum force was 5 mg. (*D*) Comparison of bolting plants that were untouched or were touched by cotton swab. (*Left*) Box-and-whisker plots of bolting days. The numbers of the total individual plants (*n*) and means ± SE from three biological replicates ($n \geq 20$ plants per replicate) are noted below and above the plots, respectively. (*Right*) Photographs of representative untouched and touch-treated plants. The results of each replication are shown in *SI Appendix*, Fig. S2. Similar results obtained from various touch treatments are shown in *SI Appendix*, Figs. S3–S5.

performed with aerial tissues. As a result, this 4C quantitative PTM proteomics (44) allowed us to identify 4,895 repeatable ($n \geq 2$) and nonredundant (herein referred to as "unique") phosphopeptides derived from 2,426 phosphoprotein groups [Datasets S1–S3; false-discovery rate (FDR) <1%, Mascot delta score ≥10; see *SI Appendix, Supplementary Materials and Methods*], which included 4,616 singly, 268 doubly, 9 triply, and 2 quadruply phosphorylated peptides. Among them, 579 phosphopeptides represented previously unreported phosphosites of the 509 protein groups (Datasets S1 and S2) according to the phosphopeptide repertoire of the PhosPhAt 4.0 database (phosphat.uni-hohenheim.de). The number of unique phosphopeptides detected from two replicates was 50% higher than that from a single replicate (3,362 vs. 2,237), whereas the number increased by only 4% (from 4,712 to 4,895) when the total number of unique phosphopeptides from six replicates was compared with that from five replicates (Fig. 2*A*). These results indicate that increasing the number of replicates to more than five contributed little to the total number of unique phosphopeptides identified using the current quantitative phosphoproteomics approach. Although over 80% of the phosphopeptides were detected in both the untouched and touch-treated samples, the number of touch-specific phosphopeptides (603) was much (2.4-fold) higher than the number of phosphopeptides specific to the untouched control (250) (Fig. 2*B*). According to the substrate sequence specificity of Ser/Thr protein kinases (45), 28%, 9%, and 27% of the phosphorylated Ser/Thr are found in acidophilic ($_p$[S/T][D/E] or $_p$[S/T]xx[D/E]), basophilic (Rxx$_p$[S/T]), and proline-directed ($_p$[S/T]P) motifs, respectively (Fig. 2*C*). Moreover, we identified six touch-specific phosphorylation motifs via bioinformatics analysis of the phosphoproteome (*SI Appendix*, Fig. S7), suggesting that some touch-regulated phosphorylation events may be catalyzed by related kinases.

We also performed quantitative PTM proteomic analysis of the ratios of isotope-coded peptides in 750 strictly selected, quantifiable pairs of light and heavy phosphopeptides (see *SI Appendix, Supplementary Materials and Methods* and Dataset S3 for selection criteria), leading to the identification of 23 touch-enhanced phosphopeptides and one touch-suppressed phosphopeptide (Fig. 2*D* and *SI Appendix*, Fig. S8 and Table S1), corresponding to a total of 24 phosphoprotein groups (in which several phosphoproteins may share the same phosphopeptide). The largest phosphorylation increase was obtained on phosphopeptides $_{23,25}$FLTQSG***p*T**FKDGDLR (15.2-fold; ***p*T**, phosphorylated threonine), derived from MAP KINASE KINASE1 [MKK1, The Arabidopsis Information Resource (TAIR) AT4G26070] and/or MKK2 (TAIR AT4G29810), and the greatest decrease (−1.4-fold) of phosphorylation occurred on $_{20}$LSPAASEVFG***p*T**GR from the light-harvesting chlorophyll–protein complex II subunit B1 (LHB1B1, TAIR AT2G34430). These SILIA-based quantitative PTM proteomic results are consistent with the observed difference in the number of phosphopeptides obtained from the differential PTM proteomic analysis of both control and touch-treated samples (i.e., touched > untouched phosphopeptides in phosphopeptide number) (Fig. 2*B*). Therefore, the touch treatment increased both the species and phosphorylation levels of phosphopeptides. This list of selected phosphopeptides (*SI Appendix*, Table S1) includes MKK1 and/or MKK2, CALCIUM-DEPENDENT PROTEIN KINASE1 (CPK1, TAIR AT5G04870), CALMODULIN-DOMAIN PROTEIN KINASE5/6 (CPK5/6, TAIR AT4G35310/AT2G17290), and PROTEIN PHOSPHATASE 2C (PP2C) family proteins, which are known protein phosphorylation/dephosphorylation enzymes that function in cell signaling (46). In addition, the levels of two similar peptides, VN***p*S**LLSIPR and VN***p*S**LVQLPR (derived from distinct members of the PP2C family), increased 1.8- and 1.4-fold, respectively, in response to touch treatment. These results, in combination with the results of the bioinformatics analysis, revealed a conserved touch-regulated phosphosite motif in PP2C family proteins (Fig. 2*E*). Finally, we identified eight touch-enhanced phosphopeptides from eight phosphoproteins of unknown function, which we named "touch-regulated phosphoproteins," TREPHs (*SI Appendix*, Table S1). Bioinformatic analysis of the touch-regulated phosphosites predicted a number of putative touch-regulated phosphosites; one of these motifs is the S625 phosphosite motif of TREPH1, which shares sequence similarity with putative phosphosites in RECEPTOR-LIKE PROTEIN 47 (RLP47,

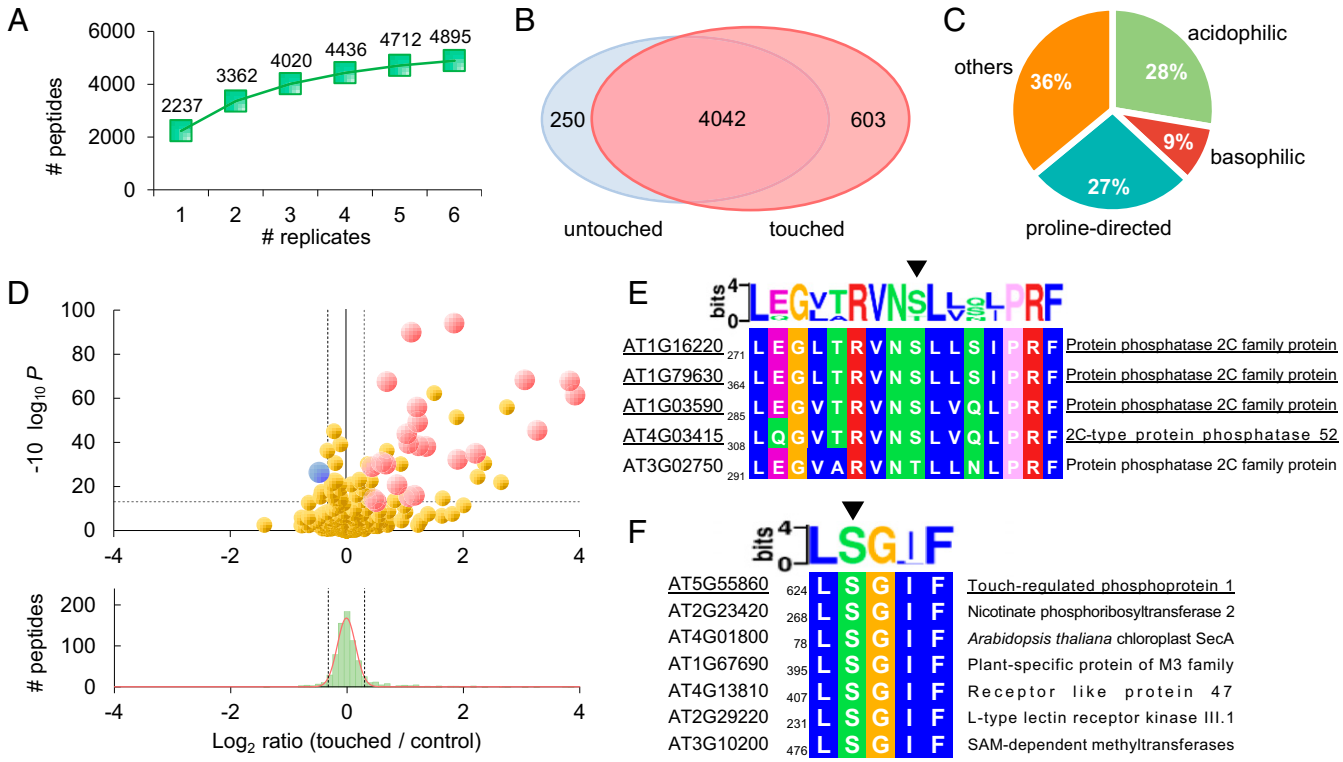


**Fig. 2.** Quantitative phosphoproteomic identification of touch-responsive phosphoproteins. (*A*) The average number of unique phosphopeptides observed from the combination of different sets of experimental replicates. Each replicate consisted of a mixture of $^{14}$N- and $^{15}$N-labeled proteins. The detailed SILIA framework is shown in *SI Appendix*, Fig. S6. (*B*) The sizes of the untouched and touch-specific phosphopeptides and their overlap (Datasets S1 and S2). (*C*) Classification of phosphorylation sites in three general categories according to kinase docking site amino acid sequence specificity. (*D*) Volcano plots of quantitative phosphopeptide analysis. (*Upper*) The red and blue circles represent significantly touch-enhanced and -suppressed phosphopeptides, respectively, defined by *t* test followed by Benjamini–Hochberg correction. The log2 ratio is the average binary logarithmic ratio of MS1 isotopologue areas of a phosphopeptide between touch-treated and control plants (Dataset S3), and *P* is the *P* value determined using Student's *t* test followed by Benjamini–Hochberg multiple hypothesis test correction. The horizontal dashed line indicates the cutoff threshold for the significance ($FDR_{B.-H.} \leq 5\%$). (*Lower*) The histogram shows the log2 ratios, which were fitted using a normal distribution (red curve). In both panels, the vertical black dashed lines indicate the mean distribution ± 2 SD of the log2 ratios of all phosphopeptides. (*E*) Highly conserved touch-regulated phosphosite motifs. VN***p*S**LLSIPR and VN***p*S**LVQLPR, the touch-enhanced phosphopeptides of PP2C family members, were used to construct a WebLogo of a touch-regulated motif from the highly conserved amino acid sequences surrounding the phosphosites and those identified from amino acid sequence BLAST searching. (*F*) The BLAST-based phosphosite motif predicted from phosphosite S625 of TREPH1 protein. In *E* and *F*, TAIR accessions and annotations are labeled on both sides of the peptides. The subscript numbers before the peptide sequences indicate the positions of the first amino acid residues in the corresponding proteins. Triangles (▼) indicate the phosphorylation sites. The experimentally identified phosphoproteins are underlined.

TAIR AT4G13810) and L-TYPE LECTIN RECEPTOR KINASE III.1 (LECRK-III.1, TAIR AT2G29220) (Fig. 2*F*). These results suggest that these putative kinases might play a role in plant touch responses.

**Confirmation of Touch-Regulated Protein Phosphorylation.** To investigate the molecular functions of candidate phosphoproteins, we first performed bioinformatic analysis of the touch-regulated phosphoproteins listed in *SI Appendix*, Table S1. Interestingly, we identified two protein–protein interactomic modules using the STRING program (*SI Appendix*, Fig. S9*A*). One module is mainly composed of kinases and phosphatases of the MAPK cascade interconnected with the $Ca^{2+}$-dependent kinase-mediated phosphor-relay pathway (*SI Appendix*, Fig. S9*A*). Another module shares related components of mechano-signalosomes found in animal cells (6), which consist of dual-tethered architectural integrins that span the plasma membrane and physically interconnect the intracellular actomyosin cytoskeleton with ECM architectural fibronectin proteins (*SI Appendix*, Fig. S9*A*). Previous studies predicted that the previously uncharacterized protein TREPH1 is a WEB1/PMI2-related protein that may be a cytoskeleton component related to plastid movement (47, 48). Homology-based protein-structure prediction suggested that TREPH1 may have a sickle-shaped structure consisting of five coiled-coil domains (*SI Appendix*, Fig. S9*B*). We decided to select both TREPH1 and MKK1/2 proteins for further investigation to interrogate the two touch-related interactome modules (*SI Appendix*, Fig. S9*A*).

By quantitative PTM proteomics, TREPH1 has a relatively large (8.3-fold) increase in phosphorylation status at the S625 residue in response to touch, while MKK1/2 proteins have the greatest (15.2-fold) phosphorylation increase at the T29 site of MKK1 and/or the T31 site of MKK2 (*SI Appendix*, Table S1). To validate these changes, we generated polyclonal antibodies against both the S625-nonphosphorylated TREPH1 (anti-npTREPH1) and S625-phosphorylated TREPH1 (anti-pTREPH1) and the T29-phosphorylated MKK1 and/or T31-phosphorylated MKK2 (anti-pMKK1/2) peptides. The antibodies were validated using immuno-dot blots with synthetic peptides (*SI Appendix*, Fig. S10 *A* and *H*). Immunoblot-based quantitation of phosphorylation demonstrated that the phosphorylation of TREPH1 increased 2.4 ± 0.2-fold in response to touch (Fig. 3*A* and *SI Appendix*, Figs. S10*B* and S11*A*), and TREPH1 phosphorylation was sustained after a 40-s cotton-swab touch (Fig. 3*B* and *SI Appendix*, Figs. S10*C* and S11*B*).

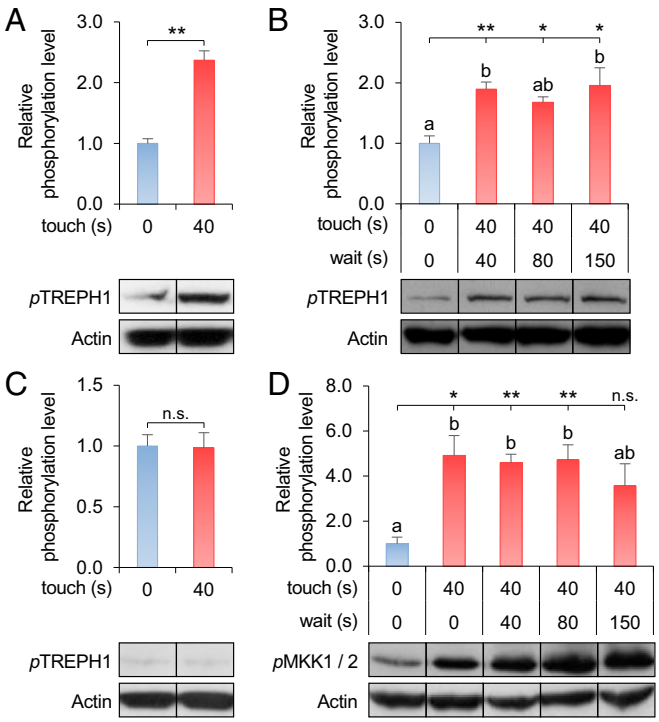


**Fig. 3.** Protein immunoblot analysis of the touch-regulated phosphorylation of MKK1/2 and TREPH1. (*A*) The enhanced phosphorylation level of TREPH1 after 40-s cotton-swab touch treatment. (*B*) Time-dependent changes in the phosphorylation of S625 of TREPH1. (*C*) Negative control of TREPH1 S625 phosphorylation antibody in touch-treated *treph1-1*. (*D*) Time-dependent changes in the phosphorylation of T31 of MKK2 (and/or T29 of MKK1) after 40-s cotton-swab touch treatment. Each bar represents the results of three immunoblotting analyses (three biological replicates). Means ± SE are shown: $*P < 0.05$, $**P < 0.01$, and n.s. (nonsignificant) $P \geq 0.05$; pairwise Student's *t* test. The homogeneity of variance in each panel with multiple (more than two) values was analyzed using Tukey's range test. Different letters represent significant differences at the 5% level. The nonadjacent lanes from the same and whole immunoblot membranes are shown in *SI Appendix*, Fig. S10, and the multiple biological replicates for each immunoblot data point are shown in *SI Appendix*, Fig. S11. The genotypes of mutants were validated and are shown in *SI Appendix*, Fig. S12.

In contrast, the touch-induced phosphorylation of TREPH1 was either undetectable or fairly low in the untouched wild-type plants and in the transfer DNA (T-DNA) insertional mutant *treph1-1* (Fig. 3*C* and *SI Appendix*, Figs. S10*D* and S11*C*; see *SI Appendix*, Fig. S12 for genotyping details). The phosphorylation level of MKK1/2 also increased (4.9 ± 0.9-fold) and was maintained after a 40-s cotton-swab touch (Fig. 3*D* and *SI Appendix*, Figs. S10*E* and S11*D*). MKKI1/2 phosphorylation appears to occur very rapidly, with phosphoprotein increases detected immediately after the touch stimulus (Fig. 3*D*). Taken together, both quantitative PTM proteomics and immunoblot analysis demonstrated a rapid alteration in phosphorylation occurring in both TREPH1 and MKK1/2 upon touch induction.

**TREPH1 Is Required for the Touch-Induced Bolting Delay.** Because TREPH1 is a previously uncharacterized protein, unlike MKK1/2, we sought to focus our in-depth analysis on TREPH1, anticipating insights into the plant mechanotransduction process. Bioinformatics analysis with STRING indicates that two touch-regulated protein networks may exist (*SI Appendix*, Fig. S9*A*). TREPH1 may play a role in the cytoskeleton network mediating mechanotransduction. Homology-based tertiary structure prediction suggests that TREPH1 may consist of five tandemly arranged three-helix coiled-coil domains, have a sickle-shaped structure, and lack a transmembrane domain (*SI Appendix*, Fig. S9*B*). It was predicted that TREPH1 is a putative coiled-coil protein that may function in plastid movement-related protein–protein interactions (48). Available gene-expression data (ePlant, bar.utoronto.ca/eplant/) indicate that *TREPH1* expression is relatively constitutive in the plant life cycle, suggesting a persistent production of TREPH1 in plant cells. BLAST analysis of the TREPH1 amino acid sequence against the proteomes of both plants and animals revealed potential homologs of the TREPH1 C terminus in mammals, monocots, and dicots (*SI Appendix*, Fig. S9*C*), suggesting that TREPH1 function may be conserved in diverse organisms.

To examine whether TREPH1 has functional relevance in plant thigmomorphogenesis, we assessed touch-induced thigmomorphogenesis in a TREPH1 T-DNA insertional line, *treph1-1*. A full-length *TREPH1* transcript was undetectable in *treph1-1* plants (*SI Appendix*, Fig. S12). Protein extracts from *treph1-1* plants also showed only faint immunoreactivity to the anti-pTREPH1 antibodies and failed to show an increase in band intensity upon touch stimulation (Fig. 3*C*) compared with protein extracts from wild-type plants (Fig. 3*A*).

The *treph1-1* mutant showed a conspicuous defect in the touch-induced delay of bolting compared with that of *Col-0* wild-type plants when subjected to either cotton-swab or automated human hair touch treatments (Fig. 4 and *SI Appendix*, Fig. S13). *Col-0* plants exhibited 2.0 d of bolting delay in response to cotton-swab touch treatment (Fig. 4*A* and *SI Appendix*, Fig. S13*A*), whereas no significant delay of bolting was observed in *treph1-1* plants under these conditions (23.3 ± 0.2 d vs. 23.5 ± 0. 2 d) (Fig. 4*C* and *SI Appendix*, Fig. S13*C*). Similarly, *Col-0* plants exhibited 1.4 d of delay in bolting time (Fig. 4*B* and *SI Appendix*, Fig. S13*B*) in response to automated touch treatment, whereas delayed bolting was not observed in *treph1-1* plants (24.0 ± 0.2 d vs. 23.8 ± 0.1 d) (Fig. 4*D* and *SI Appendix*, Fig. S13*D*). Similarly, our preliminary data have shown that the loss-of-function mutants *mkk2* and *mkk1* also exhibit defects in delayed bolting in response to automated touch treatment (*SI Appendix*, Fig. S14). These touch-response mutants were not studied further for reasons explained above.

Two other phenotypic changes associated with the *Arabidopsis* touch response and thigmomorphogenesis are changes in inflorescence stem height and average rosette radius (2). Both inflorescence stem height and average rosette radius were significantly affected by touch treatment in *treph1-1* plants, but the magnitude of these responses was reduced relative to similarly treated *Col-0* plants (*SI Appendix*, Fig. S15). Overall, these results demonstrated that *treph1-1* plants are defective in touch-induced delay of bolting, and therefore *TREPH1* is essential for this aspect of thigmomorphogenesis.

**The Roles of TREPH1 in Mechanosignaling.** Since in response to touch plant cells generate cytoplasmic calcium spikes (42) implicated in touch-inducible gene expression (2), we measured the luminescence emitted from the BRET-based *GFP::Aequorin* fusion protein (G5A) (49) in both *G5A/Col-0* and *G5A/treph1-1* transgenic plants following touch treatments. The cytoplasmic calcium signals became stronger as the duration of touch treatment increased (Fig. 5*A*). No significant difference in calcium signature was observed between plants in the *Col-0* versus *treph1-1* background in response to 1-, 10-, 20-, 40-, and 60-s touch treatments (Fig. 5*A*), indicating that TREPH1 does not function upstream of the touch-induced cellular calcium signal. In *Col-0* plants, the signal strength appeared to saturate after 40 s. These results are consistent with the dose-dependent morphological changes described above (Fig. 1*A*).

To investigate whether TREPH1 may be essential for touch-induced changes in gene expression, we compared touch-regulated transcript accumulation in wild-type and *treph1-1* plants. In wild-type plants, we identified 418 genes that were up-regulated by touch

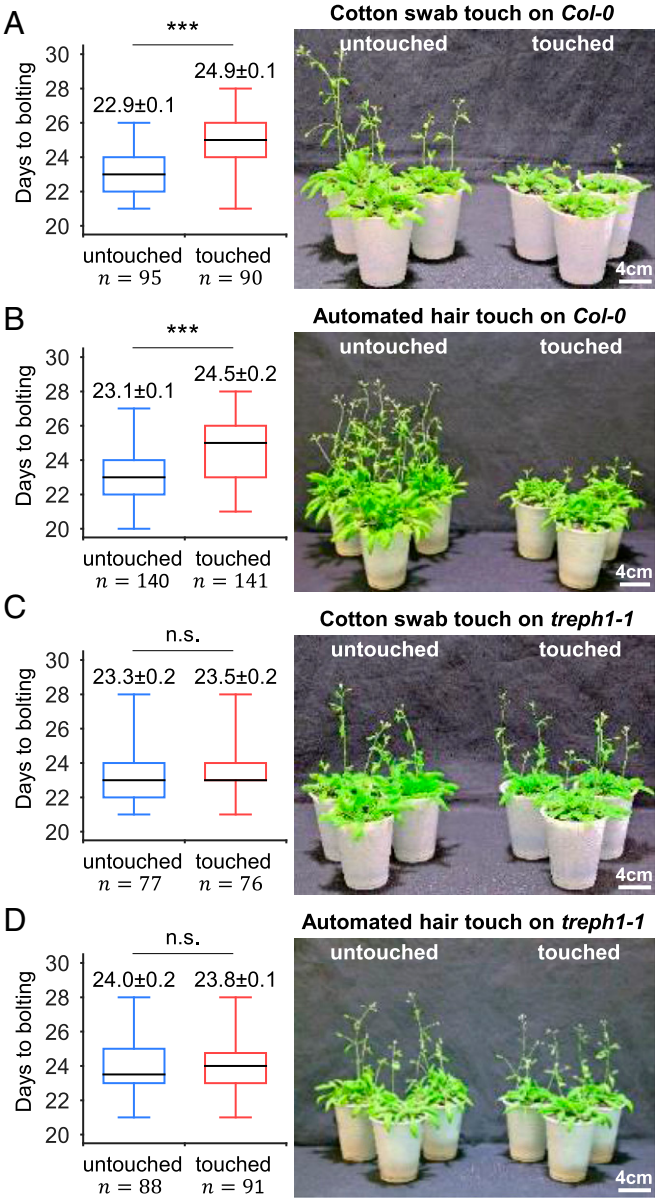


**Fig. 4.** Touch responses of wild-type, mutant, and transgenic plants expressing the TREPH1 isoforms. Box-and-whisker plots (*Left*) and representative individuals (*Right*) for the untouched control and cotton swab-touched *Col-0* (*A*), automated human hair-touched *Col-0* (*B*), cotton swab-touched *treph1-1* (*C*), and automated human hair-touched *treph1-1* (*D*) experiments. The numbers of the total individual plants (*n*) and means ± SE from three biological replicates are noted below and above the plots, respectively. The results for each replicate are shown in *SI Appendix*, Fig. S13. The genotype validation of these lines is shown in *SI Appendix*, Fig. S12. All results were compiled from three biological replicates, with $n \geq 24$ plants per replicate. Significance between the untouched and touch-treated groups of each experiment was obtained by *t* test: ***$P < 0.001$ and n.s. (not significant) $P > 0.05$.

(fold change ≥2 and probability ≥0.8) and 87 that were down-regulated by this treatment (fold change equal to or less than −2 and probability ≥0.8). We compared the transcriptomes with previous transcriptomics results, finding that 92% (47 of 51) of previously identified touch-regulated genes (43) were again detected by our RNA deep sequencing. By contrast, only 47% (76 of 162) of the genes up-regulated by wounding (50) were identified among these touch-regulated genes.

Using the type 1 ($|\Delta\log_2\text{ratio}| \geq 1$) and type 2 methods of transcriptomic analysis (*SI Appendix*, *Supplementary Materials and Methods*) to analyze the data, we identified genes that showed differential touch-responsiveness in *treph1-1* compared with wild-type plants. Genes whose expression was either up- or down-regulated by touch in wild-type plants but were less responsive in *treph1-1* plants were defined as "*TREPH1*-dependent" genes. The type 1 and type 2 methods revealed 92 and 75 *TREPH1*-dependent touch-responsive genes, respectively. Of the 167 touch-responsive genes analyzed, 67 were identified by both the type 1 and type 2 methods (Fig. 5 *B* and *C*, *SI Appendix*, Fig. S16, and Dataset S4). Of these 100 unique touch-responsive and *TREPH1*-dependent genes, 86 (86% of 100 genes) had increased expression in *treph1-1* plants, suggesting that their expression is suppressed by TREPH1 protein during the touch response, whereas 14 touch-responsive genes showed reduced expression in *treph1-1* plants, indicating that TREPH1 is required for the appropriate expression of these 14 genes. We subjected several of these genes to RT-qPCR analysis, including *CALMODULIN-LIKE38* (*CML38*, TAIR AT1G76650), *ETHYLENE RESPONSE FACTOR11* (*ERF11*, TAIR AT1G28370), and *JASMONATE-ZIM-DOMAIN PROTEIN7* (*JAZ7*, TAIR AT2G34600) found by the type 1 method as well as an unknown touch-inducible gene (*TCH2K1*, TAIR AT1G56660) found by the type 2 method (Fig. 5 *D*–*G*). *CML38*, which was reported as a touch-inducible gene in a previous study (43), and *CML39* (TAIR AT1G76640), which was reported as a touch-induced gene in the same study (43) but was not TREPH1-regulated according to our transcriptomic results, were also included as controls for touch-inducible genes (Fig. 5*H*). Although we detected a higher number of genes with increased expression levels in *treph1-1* plants (86 of 100) than in wild-type plants, no gene was selected from this group for RT-qPCR because most (73%) of these genes are implicated in energy pathways (19 photosynthetic proteins, 13 NADH dehydrogenases, 7 ATP synthases/ATPases, and 1 cytochrome) or protein synthesis (23 ribosomal proteins) (Dataset S4). Therefore, these genes are suspected to play only an indirect role, at most, in plant touch response. We thus decided not to pursue the functions of these genes at this time.

*CML38* expression was induced 36.7 ± 3.6- and 6.5 ± 0.5-fold at 5 min after the application of a 40-s touch stimulation in wild-type and *treph1-1* plants, respectively, compared with its expression at 0 min (Fig. 5*D*). *CML38* expression peaked at a level 328.5 ± 48.8- and 45.3 ± 5.4-fold that of the control at 15 min after touch induction and decreased to 31.7 ± 9.6- and 5.5 ± 1.0-fold at 60 min after touch induction in the wild-type and *treph1-1* plants, respectively. The expression pattern of *ERF11* was similar to that of *CML38*, increasing 111.3 ± 7.6- and 33.7 ± 2.5-fold in wild-type and *treph1-1* plants, respectively, at 15 min after touch induction (Fig. 5*E*). The other two touch-inducible genes, *JAZ7* and *TCH2K1*, showed similar induction kinetics within 60 min following 40-s of touch treatment in the RT-qPCR–based touch-response assay (Fig. 5 *F* and *G*). On the other hand, wild-type and *treph1-1* plants demonstrated no significant difference in *CML39* expression 15 min after touch stimulation in the transcriptomic analysis, but the genotypes showed distinct regulation (4.6 ± 0.6-fold vs. 14.8 ± 1.9-fold, respectively) of *CML39* expression 30 min after touch treatment (Fig. 5*H*).

**The Amino Acid Residue Modified by Phosphorylation in TREPH1 Is Required for Touch-Induced Delay of Flowering and Gene-Expression Changes.** Our data indicate that *TREPH1* is essential for *Arabidopsis* to respond to force stimulation by delayed bolting. We next sought to investigate the potential role of S625 phosphorylation of TREPH1 in this aspect of touch response. Therefore, we compared the performance of TREPH1 with and without the phosphorylatable S625 amino acid. We generated two transgenes for

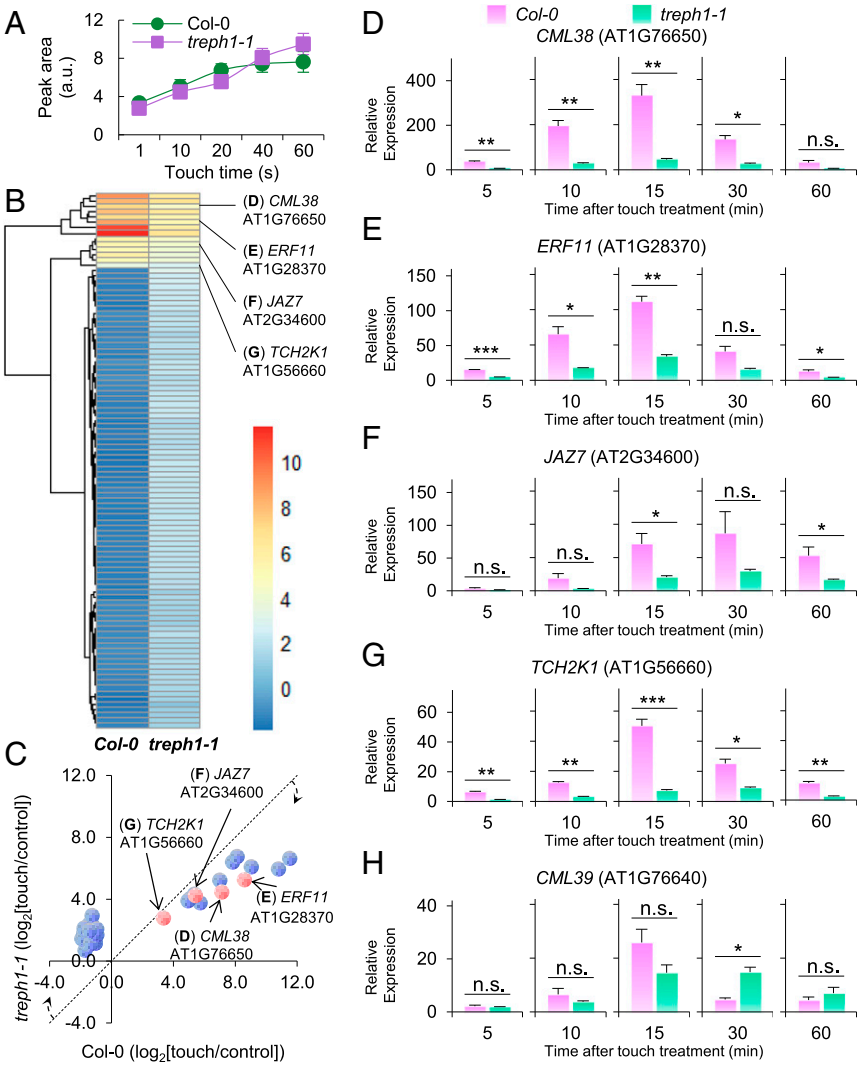


**Fig. 5.** The effects of TREPH1 in signaling and transcriptional regulation during mechanotransduction. (*A*) The relative peak areas of bioluminescence emitted from the recombinant G5A protein upon various lengths (in seconds) of touch treatments. Means ± SE are shown ($n \geq 10$ individuals). (*B*) Presentation of the log2 ratios of transcriptomic changes in wild-type *Col-0* and *treph1-1* mutant plants after a 10-min time lag following the initial 40-s touch (1 s per touch) (Dataset S4). An alternative representation of transcriptomic differences between the wild-type and mutant plants is shown in *SI Appendix*, Fig. S16. Only the transcripts showing touch-induced alterations between the wild-type and *treph1-1* mutant plants are included in both figures. Black lines point to the four genes selected for RT-qPCR analysis shown in *D*–*G*. The gradient from blue to red indicates log2 ratios ranging from −1.9 to 11.5. (*C*) The log2 ratios of transcriptomic changes in wild-type *Col-0* plants against those in *treph1-1* mutant plants after a 10-min time lag following the initial 40-s touch. The two columns of data for wild-type and *treph1-1* plants shown in *B* are plotted. The dashed straight line is the bisector line of the quadrants. The dashed arrows indicate the shift of log2 ratios between wild-type and *treph1-1* plants. The red nodes are the four genes selected for RT-qPCR analysis shown in *D*–*G*. (*D*–*H*) The expression of *CML38* (TAIR AT1G76650) (*D*), *ERF11* (TAIR AT1G28370) (*E*), *JAZ7* (TAIR AT2G34600) (*F*), *TCH2K1* (TAIR AT1G56660) (*G*), and *CML39* (TAIR AT1G76640) (*H*) was induced within 1 h after 40-s cotton-swab touch treatment in *Col-0* and *treph1-1* plants. The mRNA levels were quantified using RT-qPCR. Means ± SE of three biological replicates are shown. Statistical analysis was performed by Student's pairwise *t* test: $*P < 0.05$, $**P < 0.01$, $***P < 0.001$, and n.s. (nonsignificant) $P \geq 0.05$.

complementation tests of *treph1-1* (*SI Appendix*, Fig. S17): *dPro35S::His::YFP::TREPH1*, which retains the capability of being phosphorylated (*SI Appendix*, Fig. S10*G*), and *dPro35S::His::YFP::TREPH1*$^{S625A}$, which removes the phosphorylatable amino acid. These transgenes were introduced into *treph1-1* plants. In the presence of *dPro35S::His::YFP::TREPH1*, the touch-induced bolting delay of *treph1-1* was rescued. Cotton swab-touched plants bolted with an average of 24.7 ± 0.2 d, whereas untouched plants bolted at 23.4 ± 0.1 d (Fig. 6*A* and *SI Appendix*, Fig. S18*A*). Automated human hair touch delayed the average bolting time from 23.7 ± 0.1 d to 24.8 ± 0.1 d (Fig. 6*B* and *SI Appendix*, Fig. S18*B*). However, the *dPro35S::His::YFP::TREPH1*$^{S625A}$-complemented population showed no significant delay in bolting (23.3 ± 0.1 d vs. 23.5 ± 0.1 d and 25.4 ± 0.1 d vs. 25.3 ± 0.1 d for trials using cotton swabs and automated human hair, respectively) (Fig. 6 *C* and *D* and *SI Appendix*, Fig. S18 *C* and *D*). Thus, the transgenic wild-type TREPH1 protein, but not the point-mutated TREPH1$^{S625A}$ protein, can rescue touch-induced delayed bolting (Fig. 6 *A*–*D*). Therefore, the S625 amino acid of TREPH1 is required for TREPH1's function in delayed bolting in response to touch.

We also performed RT-qPCR analysis in transgenic populations of *dPro35S::His::YFP::TREPH1*/*treph1-1* and *dPro35S::His::YFP::TREPH1*$^{S625A}$/*treph1-1* plants to determine whether S625 phosphorylation of TREPH1 is required for the expression of touch-regulated genes (Fig. 6*E*). Although the presence of the *dPro35S::His::YFP::TREPH1* transgene rescues the *treph1-1* touch expression inducibility of the genes tested, the presence of the *dPro35S::His::YFP::TREPH1*$^{S625A}$ in the *treph1-1* background resulted in significantly reduced expression levels of *CML38*, *ERF11*, *JAZ7*, and *TCH2K1* but not *CML39* (Fig. 6*E*). Taken together, these results demonstrate a critical role for S625 in the functioning of the TREPH1 protein both in regulating the touch-induced delay of bolting and in touch-induced gene expression, suggesting the possibility that the touch-induced phosphorylation of TREPH1 is an essential step in the touch-response pathway of *Arabidopsis*.

To gain some insight into how TREPH1 may function, we sought to determine whether the TREPH1 protein may associate with cellular membranes. We separated cellular extracts into membrane and soluble fractions, followed by immunoblot analysis using both anti-npTREPH1 and anti-pTREPH1 antibodies (Fig. 6*F*). Both antibodies detected protein in the soluble fraction and not in the membrane fraction, consistent with TREPH1 likely being a cytosolic protein.

To verify that the mechanical stimulus, rather than any other effects in our touch treatment, was the causal inducer, we also analyzed TREPH1 phosphorylation in response to gloved finger touch, air blowing (mimicking wind force), and water sprinkling (resembling rainfall force). A 40- or 150-s gloved-finger touch of wild-type plants led to a 2.9 ± 0.3- and 2.3 ± 0.2-fold increase in

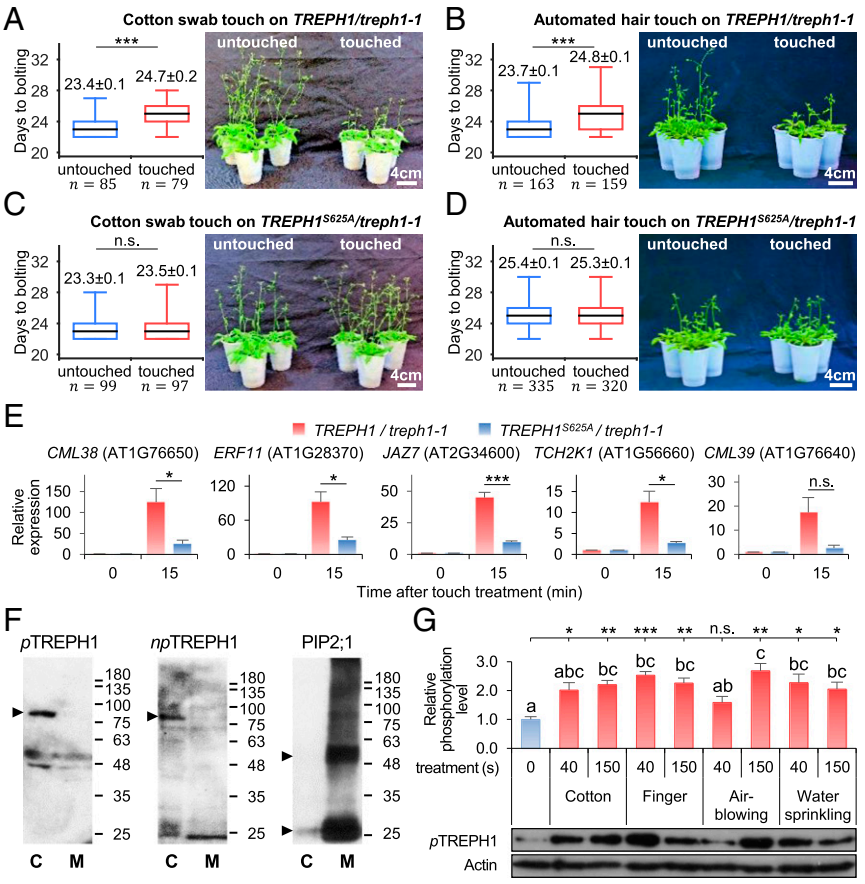


**Fig. 6.** Analysis of the key roles of TREPH1 in mechanotransduction. (*A–D*) Box-and-whisker plots (*Left*) and representative individuals (*Right*) for the untouched control and cotton-swab–touched *TREPH1/treph1-1* (*A*), automated human hair-touched *TREPH1/treph1-1* (*B*), cotton-swab–touched *TREPH1*$^{S625A}$/*treph1-1* (*C*), and automated human hair-touched *TREPH1*$^{S625A}$/*treph1-1* (*D*) plants. Details of transgenes and the results of each replication are shown in *SI Appendix*, Figs. S17 and S18, respectively. (*E*) Changes in mRNA abundance of *CML38*, *ERF11*, *JAZ7*, *TCH2K1*, and *CML39* induced by 40-s cotton-swab touch treatment in *TREPH1/treph1-1* and *TREPH1*$^{S625A}$/*treph1-1* transgenic plants. (*F*) Biochemical analysis of cytosolic (C) and integral membrane (M) protein fractions in wild-type plant cells. Immunoblots from left to right show anti-pTREPH1, anti-npTREPH1, and anti-PIP2;1 immunoblotting, respectively. Arrowheads at the left of the immunoblots indicate the target protein bands. Antibody specificity is shown in *SI Appendix*, Fig. S10 *A* and *H*. (*G*) Changes in phosphorylation levels at S625 of TREPH1 in *Arabidopsis* plants touched with a cotton swab or a finger, treated with air blowing, or treated with water sprinkling. The plants were grown for 3 wk in soil. Each bar represents the results of three biological replicates. Means ± SE are shown. Statistical analysis was performed by Student's *t*-test and Tukey's range test. Significance at $P < 0.05$, $P < 0.01$, $P < 0.001$, and $P \geq 0.05$ for pairwise *t*-test are shown as *, **, ***, and n.s., respectively. The homogeneity of variance in each panel with multiple (more than two) values was analyzed using Tukey's range test. Different letters represent significant differences at the 5% level.

pTREPH1, respectively (Fig. 6*G* and *SI Appendix*, Figs. S10*F* and S11*E*). Similarly, TREPH1 phosphorylation increased by 3.1 ± 0.3-fold in response to 150-s air blowing and by 2.3 ± 0.3- and 2.0 ± 0.2-fold, respectively, in response to 40- and 150-s water-sprinkling treatments (Fig. 6*G* and *SI Appendix*, Figs. S10*F* and S11*E*). Thus, TREPH1 S625 phosphorylation is responsive to diverse mechanostimuli, suggesting a potential role in diverse environmental force loadings, including rain and wind.

## Discussion

The machinery responsible for mechanosensitivity, including bona fide mechanosensitive channels and multimeric mechanosignalosomes, is believed to have evolved multiple times during flowering plant evolution (22). Numerous force sensors may coordinate multiple levels of mechanical signaling originating from intracellular molecular activities and extracellular mechanical signals during versatile plant mechanoresponses (51). One group of sensors includes the mechanosensitive divalent and monovalent ion channels (5), such as MSL, MCA, Piezo, and TPK, and the other group comprises membrane-bound receptor-like wall-associated kinases (WAKs) and other receptor-like kinases (RLKs) (37–39). These kinases span the plasma membrane, with one terminal domain linked to the extracellular cell wall and the other terminal domain harboring a cytoplasmic kinase. RLKs are thought to function as kinase activity-associated mechanosensitive sensors that regulate downstream calcium transients or directly transduce a mechanical phosphor-relay to nuclear events (37). The mechanical signal-induced $[Ca^{2+}]_{cyt}$ signature has a time scale ranging from 5 s to several minutes (42, 52). Calcium-dependent protein kinases (CDPKs) and calcium-binding proteins (CBPs) are thought to respond to force signals at the time of the initial touch treatment (40), and these CDPKs might trigger protein phosphorylation within seconds. It therefore is plausible that protein phosphorylation, one of the most abundant post-translational modifications (53), may act to transduce mechanosignals in an ion channel-dependent and/or -independent fashion. Our discovery of 24 rapidly mechanoresponsive phosphosites of protein groups (*SI Appendix*, Table S1) supports this view.

Like membrane-bound mechano-signalosomes found in animals (6, 35), kinases may be part of the force-sensing signalosomes in plants and may span the plasma membrane and be tethered to the ECM or cell wall and to the cytoskeleton, enabling perception of the deformation and plasma membrane tension imposed by mechanical forces such as touch. For example, a 500-kDa WAK1 protein complex contains a WAK1 kinase subunit, a glycine-rich extracellular protein subunit, an AtGRP-3, and a cytoplasmic type 2C protein phosphatase, KAPP, which can associate with a Rho-related protein (54–56). Interestingly, we also found that kinases/phosphatases MKK1/2, CPK1, CPK5/6, and four PP2C family proteins, as well as the cytoskeletal protein XIK and kinesin-like (KAC1) and tubulin (TUA1/2/4/6) proteins, were among the rapidly and highly phosphorylated proteins identified after a 40-s force-loading treatment (*SI Appendix*, Fig. S9*A* and Table S1). These rapid changes upon mechanostimulation suggest the possibility that these phosphoproteins associated with the two protein interactomic modules (*SI Appendix*, Fig. S9) identified by the STRING program may play roles in early force signaling in plant cells.

The 4C quantitative PTM proteomics generally produces a series of candidate proteins with an arbitrarily defined confidence level (for example, 95% of positive rate, as used to select the touch-regulated

phosphosites shown in *SI Appendix*, Table S1). As a result, an acceptable small percentage of false-positive results (≤5%) is usually present among the selected phosphoproteins (FDR after the Benjamini–Hochberg correction, hereafter $FDR_{B.-H.}$, ≤5%). Biochemical, genetic, and physiological characterizations of candidate proteins complement -omics approaches to provide confirmation of the 4C quantitative PTM proteomics. In this proteomic study, the application of Benjamini–Hochberg hypothesis test correction has allowed us to select 24 touch-regulated phosphosites with a 5% $FDR_{B.-H.}$ cutoff to focus on a small set of mutants to screen for defective touch responses. We screened eight homozygous T-DNA insertional mutant lines of putative touch-regulated phosphoprotein-encoding genes, including *treph1-1*, *mkk1*, and *mkk2*. These putative touch-regulated phosphoproteins were selected based on their relatedness to two bioinformatics-predicted interactomic modules (*SI Appendix*, Fig. S9*A*) their previously documented functions and/or expression behaviors, and their high phosphorylation levels confirmed by both PTM proteomics quantitation and immunoblot analysis. During this preliminary genetic screen for thigmomorphogenesis defects, we found that homozygous *mkk1* and *mkk2* mutants displayed a putative defective bolting-delay phenotype, suggesting that MKK1/2 may also play roles in this aspect of the *Arabidopsis* touch response (*SI Appendix*, Fig. S14).

In this study, we focused on characterizing a protein, TREPH1, to initiate functional studies on touch-regulated phosphoproteins. We demonstrated that TREPH1 is required for both a salient developmental response to touch in plants, i.e., bolting time (Fig. 4), and for touch-regulated gene expression (Fig. 5). Furthermore, both of these TREPH1 functions require the presence of S625, the amino acid that becomes phosphorylated upon touch, because TREPH1 protein isoforms with an alanine substitution at position 625 are unable to rescue the *treph1-1* mutant touch-dependent phenotypes (Fig. 6). These data demonstrate a critical role for TREPH1 and implicate TREPH1 phosphorylation in *Arabidopsis* mechanoresponses.

A dynamic change at the gene-expression level is associated with the morphological changes that occur during the plant touch response (2, 4, 57). Many genes are transiently altered in expression, with transcript levels changing within 5 min upon touch treatment, peaking between 10–30 min, and returning to basal levels within 1–2 h (Fig. 5) (58, 59). In the present study, we found that the touch-triggered phosphorylation events occurred within 40 s and coincided with luminescence reporting of cytoplasmic calcium ion levels. TREPH1 is not required for touch-induced changes in calcium signaling; luminescence reporting of intracellular calcium levels shows clear responses to 10- to 60-s touch treatments in *treph1-1* plants comparable to those in wild-type plants (Fig. 5*A*). These results are consistent with TREPH1 acting downstream of or in parallel with calcium signaling (*SI Appendix*, Fig. S19).

Modeling suggests that TREPH1 may have a sickle-shaped structure of five tandemly arranged three-helix coiled-coil domains and lacks a transmembrane domain (*SI Appendix*, Fig. S9*B*). Thus, TREPH1 is unlikely to be an integral membrane protein; a cytosolic localization is more likely, as demonstrated by TREPH1 being enriched in the soluble cellular fractions and absent from the membrane protein fractions (Fig. 6*F*). Intriguingly, the putative TREPH1 structure resembles the cytoplasmic domain of the bacterial cell division protein EzrA, which regulates the formation of the cytokinetic Z-ring formed by the tubulin homolog FtsZ protein (60), suggesting the possibility of potential interactions between TREPH1 and tubulin and/or FtsZ-like proteins in plant cells and thus a possible cytoskeleton-related role (*SI Appendix*, Fig. S9*A*).

It has been documented that the phosphor-relay–mediated cell-signaling components, MAP kinases and calcium-dependent protein kinases, are involved in various abiotic and biotic stress-signaling pathways (61). Our quantitative phosphoproteomic study indeed revealed touch-induced phosphopeptide changes in MKK1 and/or MKK2 phosphoproteins. These two kinases have overlapping functions in some signaling responses (62–64). However, different kinase activities of these two MKKs were also detected under various stress conditions (62, 65). For example, 10 min of 4 °C chilling treatment of plants triggered the activity of MKK1 in phosphorylating MPK4 (66), whereas 10 min of 0 °C freezing treatment induced the kinase activity of MKK2 but not MKK1 (65). Thus, it is possible that MKK1 and MKK2 may transduce force signals through overlapping and/or kinase-specific pathways, as shown in *SI Appendix*, Fig. S14.

To integrate our research results presented here with the current state of knowledge, we developed a force-signaling model for the *Arabidopsis* touch response, as shown in *SI Appendix*, Fig. S19. TREPH1, as a soluble, likely cytosolic protein, may associate with mechano-signalosomes or force-activated ion channels to transduce the touch signals downstream. The MAPK kinase cascade undergoes crosstalk with calcium-dependent protein kinases during abiotic and biotic stress signaling (61). These two touch-signaling pathways may cooperatively regulate the expression of the same group of genes that are regulated during plant growth and bolting (67, 68). ERF11 and JAZ7 transcription factors may function downstream of these signal transduction pathways. ERF11 functions in gibberellin (GA) biosynthesis, GA-regulated flowering, and ethylene biosynthesis (69). The phosphorylated isoform of ERF110 promotes bolting in *Arabidopsis*, while the overexpression of S62-nonphosphorylated ERF110 suppresses bolting (70). On the other hand, JAZ7 regulates the jasmonic acid response and flowering in *Arabidopsis* (71). Taking these findings together, we hypothesize that rapid touch-responsive kinases and phosphatases quickly modify both the expression level and PTM code of these regulators to modulate the touch response. TREPH1 has been identified as a key player in the *Arabidopsis* touch response, being required for both the developmental response of bolting time delay (Fig. 4) and the expression of key touch-inducible genes (Fig. 5).

In conclusion, proteome-wide protein phosphorylation is a rapid and broad response to touch stimulation in *Arabidopsis* and may play a critical role in the mechanoresponse pathways of plants.

## Materials and Methods

The details of plant materials, growth conditions, force treatment, the high-throughput SILIA-based quantitative phosphoproteomics approach, antibody preparation, immunoblot assay, subcellular fractionation, transcriptomics, RT-qPCR, luciferase and $Ca^{2+}$ imaging, and other bioinformatic and statistical analyses are provided in *SI Appendix, Supplementary Materials and Methods*. These methods are also briefly described in figure legends.

**ACKNOWLEDGMENTS.** We thank Dr. Marc Knight and Dr. Jean-Baptiste Thibaud for the gift of the *AEQ* gene and the GFP-Aequorin fusion gene (*G5A*), respectively; Dr. Andrew L. Miller and Ms. Mandy Chan [Division of Life Science, Hong Kong University of Science and Technology (HKUST)] for providing the custom-built platform used to perform the luminescence $Ca^{2+}$ imaging experiment; K. Y. Law, M. Y. Chen, and M. H. Leung for their contributions to touch treatments; and particularly Nicole Wong, Stacy Zhu, S. K. Cheung, and W. C. Lee for their contributions to the development of touch equipment and method for the touch responses and Jennifer Lockhart and Kathleen Farquharson for their contributions to the editing of this manuscript. This research was supported by National Science Foundation of China Grants 31370315 and 31570187; Research Grants Council of Hong Kong Grants 661613, 16101114, 16103615, 16103817, and AoE/M-403/16; Energy Institute of HKUST Grants SRF11EG17PG-A and SRFI11EG17-A; Grant SBI09/10.EG01-A from the Croucher Foundation Chinese Academy of Science-HKUST Joint Laboratory Matching Fund; the Rice 04 Sponsorship Scheme for Targeted Strategic Partnerships; and Guangdong-Hong Kong Key Area Breakthrough Program Grant GDST16SC02.

1. Morris CE, Homann U (2001) Cell surface area regulation and membrane tension. *J Membr Biol* 179:79–102.
2. Braam J (2005) In touch: Plant responses to mechanical stimuli. *New Phytol* 165: 373–389.
3. Hamant O, et al. (2008) Developmental patterning by mechanical signals in Arabidopsis. *Science* 322:1650–1655.
4. Chehab EW, Eich E, Braam J (2009) Thigmomorphogenesis: A complex plant response to mechano-stimulation. *J Exp Bot* 60:43–56.
5. Hamilton ES, et al. (2015) Mechanosensitive channel MSL8 regulates osmotic forces during pollen hydration and germination. *Science* 350:438–441.
6. Dreher D, Pasakarnis L, Brunner D (2016) SnapShot: Mechanical forces in development II. *Cell* 165:1028.e1.
7. Pasakarnis L, Dreher D, Brunner D (2016) SnapShot: Mechanical forces in development I. *Cell* 165:754.e1.
8. Hamilton ES, Schlegel AM, Haswell ES (2015) United in diversity: Mechanosensitive ion channels in plants. *Annu Rev Plant Biol* 66:113–137.
9. Uyttewaal M, et al. (2012) Mechanical stress acts via katanin to amplify differences in growth rate between adjacent cells in Arabidopsis. *Cell* 149:439–451.
10. MacCleery SA, Kiss JZ (1999) Plastid sedimentation kinetics in roots of wild-type and starch-deficient mutants of Arabidopsis. *Plant Physiol* 120:183–192.
11. Telewski FW (2006) A unified hypothesis of mechanoperception in plants. *Am J Bot* 93:1466–1476.
12. Toyota M, Gilroy S (2013) Gravitropism and mechanical signaling in plants. *Am J Bot* 100:111–125.
13. Coutand C (2010) Mechanosensing and thigmomorphogenesis, a physiological and biomechanical point of view. *Plant Sci* 179:168–182.
14. Isnard S, Silk WK (2009) Moving with climbing plants from Charles Darwin's time into the 21st century. *Am J Bot* 96:1205–1221.
15. Darwin C (1875) *Insectivorous Plants* (John Murray, London), p x, 462 p.
16. Jaffe MJ, Leopold AC, Staples RC (2002) Thigmo responses in plants and fungi. *Am J Bot* 89:375–382.
17. Jaffe MJ, Telewski FW, Cooke PW (1984) Thigmomorphogenesis: On the mechanical properties of mechanically perturbed bean plants. *Physiol Plant* 62:73–78.
18. Telewski FW, Jaffe MJ (1986) Thigmomorphogenesis: Anatomical, morphological and mechanical analysis of genetically different sibs of Pinus taeda in response to mechanical perturbation. *Physiol Plant* 66:219–226.
19. Johnson KA, Sistrunk ML, Polisensky DH, Braam J (1998) Arabidopsis thaliana responses to mechanical stimulation do not require ETR1 or EIN2. *Plant Physiol* 116:643–649.
20. Vogel M (1994) Automatic precision-measurements of radial increment in a mature spruce stand and interpretation variants of short-term changes in increment values. *Allg Forst Jagdztg* 165:34–40.
21. Boonsirichai K, Guan C, Chen R, Masson PH (2002) Root gravitropism: An experimental tool to investigate basic cellular and molecular processes underlying mechanosensing and signal transmission in plants. *Annu Rev Plant Biol* 53:421–447.
22. Bastien R, Bohr T, Moulia B, Douady S (2013) Unifying model of shoot gravitropism reveals proprioception as a central feature of posture control in plants. *Proc Natl Acad Sci USA* 110:755–760.
23. Vandenbrink JP, Kiss JZ, Herranz R, Medina FJ (2014) Light and gravity signals synergize in modulating plant development. *Front Plant Sci* 5:563.
24. Ge L, Chen R (2016) Negative gravitropism in plant roots. *Nat Plants* 2:16155.
25. Massa GD, Gilroy S (2003) Touch modulates gravity sensing to regulate the growth of primary roots of Arabidopsis thaliana. *Plant J* 33:435–445.
26. Nakagawa Y, et al. (2007) Arabidopsis plasma membrane protein crucial for Ca2+ influx and touch sensing in roots. *Proc Natl Acad Sci USA* 104:3639–3644.
27. Maathuis FJ (2011) Vacuolar two-pore K+ channels act as vacuolar osmosensors. *New Phytol* 191:84–91.
28. Maksaev G, Haswell ES (2012) MscS-Like10 is a stretch-activated ion channel from Arabidopsis thaliana with a preference for anions. *Proc Natl Acad Sci USA* 109:19015–19020.
29. Kung C, Martinac B, Sukharev S (2010) Mechanosensitive channels in microbes. *Annu Rev Microbiol* 64:313–329.
30. Delmas P, Coste B (2013) Mechano-gated ion channels in sensory systems. *Cell* 155: 278–284.
31. Coste B, et al. (2010) Piezo1 and Piezo2 are essential components of distinct mechanically activated cation channels. *Science* 330:55–60.
32. Ge J, et al. (2015) Architecture of the mammalian mechanosensitive Piezo1 channel. *Nature* 527:64–69.
33. Ernstrom GG, Chalfie M (2002) Genetics of sensory mechanotransduction. *Annu Rev Genet* 36:411–453.
34. Liu C, Montell C (2015) Forcing open TRP channels: Mechanical gating as a unifying activation mechanism. *Biochem Biophys Res Commun* 460:22–25.
35. Provenzano PP, Keely PJ (2011) Mechanical signaling through the cytoskeleton regulates cell proliferation by coordinated focal adhesion and Rho GTPase signaling. *J Cell Sci* 124:1195–1205.
36. Guo G, Li N (2011) Relative and accurate measurement of protein abundance using 15N stable isotope labeling in Arabidopsis (SILIA). *Phytochemistry* 72:1028–1039.
37. Chae L, Sudat S, Dudoit S, Zhu T, Luan S (2009) Diverse transcriptional programs associated with environmental stress and hormones in the Arabidopsis receptor-like kinase gene family. *Mol Plant* 2:84–107.
38. He ZH, Fujiki M, Kohorn BD (1996) A cell wall-associated, receptor-like protein kinase. *J Biol Chem* 271:19789–19793.
39. Verica JA, Chae L, Tong H, Ingmire P, He ZH (2003) Tissue-specific and developmentally regulated expression of a cluster of tandemly arrayed cell wall-associated kinase-like kinase genes in Arabidopsis. *Plant Physiol* 133:1732–1746.
40. Haley A, et al. (1995) Effects of mechanical signaling on plant cell cytosolic calcium. *Proc Natl Acad Sci USA* 92:4124–4128.
41. Wright AJ, Knight H, Knight MR (2002) Mechanically stimulated TCH3 gene expression in Arabidopsis involves protein phosphorylation and EIN6 downstream of calcium. *Plant Physiol* 128:1402–1409.
42. Knight MR, Campbell AK, Smith SM, Trewavas AJ (1991) Transgenic plant aequorin reports the effects of touch and cold-shock and elicitors on cytoplasmic calcium. *Nature* 352:524–526.
43. Lee D, Polisensky DH, Braam J (2005) Genome-wide identification of touch- and darkness-regulated Arabidopsis genes: A focus on calmodulin-like and XTH genes. *New Phytol* 165:429–444.
44. Yang Z, et al. (2013) Stable isotope metabolic labeling-based quantitative phosphoproteomic analysis of Arabidopsis mutants reveals ethylene-regulated time-dependent phosphoproteins and putative substrates of constitutive triple response 1 kinase. *Mol Cell Proteomics* 12:3559–3582.
45. O'Neill T, et al. (2000) Utilization of oriented peptide libraries to identify substrate motifs selected by ATM. *J Biol Chem* 275:22719–22727.
46. Hunter T (1995) Protein kinases and phosphatases: The yin and yang of protein phosphorylation and signaling. *Cell* 80:225–236.
47. Gardiner J, Overall R, Marc J (2011) Putative Arabidopsis homologues of metazoan coiled-coil cytoskeletal proteins. *Cell Biol Int* 35:767–774.
48. Kodama Y, Suetsugu N, Wada M (2011) Novel protein-protein interaction family proteins involved in chloroplast movement response. *Plant Signal Behav* 6:483–490.
49. Xiong TC, et al. (2014) Imaging long distance propagating calcium signals in intact plant leaves with the BRET-based GFP-aequorin reporter. *Front Plant Sci* 5:43.
50. Walley JW, et al. (2007) Mechanical stress induces biotic and abiotic stress responses via a novel cis-element. *PLoS Genet* 3:1800–1812.
51. Monshausen GB, Haswell ES (2013) A force of nature: Molecular mechanisms of mechanoperception in plants. *J Exp Bot* 64:4663–4680.
52. Plieth C, Trewavas AJ (2002) Reorientation of seedlings in the earth's gravitational field induces cytosolic calcium transients. *Plant Physiol* 129:786–796.
53. Derouiche A, Cousin C, Mijakovic I (2012) Protein phosphorylation from the perspective of systems biology. *Curr Opin Biotechnol* 23:585–590.
54. Park AR, et al. (2001) Interaction of the Arabidopsis receptor protein kinase Wak1 with a glycine-rich protein, AtGRP-3. *J Biol Chem* 276:26688–26693.
55. Trotochaud AE, Hao T, Wu G, Yang Z, Clark SE (1999) The CLAVATA1 receptor-like kinase requires CLAVATA3 for its assembly into a signaling complex that includes KAPP and a Rho-related protein. *Plant Cell* 11:393–406.
56. Anderson CM, et al. (2001) WAKs: Cell wall-associated kinases linking the cytoplasm to the extracellular matrix. *Plant Mol Biol* 47:197–206.
57. Braam J, Chehab EW (2017) Thigmomorphogenesis. *Curr Biol* 27:R863–R864.
58. Braam J, Davis RW (1990) Rain-, wind-, and touch-induced expression of calmodulin and calmodulin-related genes in Arabidopsis. *Cell* 60:357–364.
59. Gutierrez RA, Ewing RM, Cherry JM, Green PJ (2002) Identification of unstable transcripts in Arabidopsis by cDNA microarray analysis: Rapid decay is associated with a group of touch- and specific clock-controlled genes. *Proc Natl Acad Sci USA* 99: 11513–11518.
60. Cleverley RM, et al. (2014) Structure and function of a spectrin-like regulator of bacterial cytokinesis. *Nat Commun* 5:5421.
61. Wurzinger B, Mair A, Pfister B, Teige M (2011) Cross-talk of calcium-dependent protein kinase and MAP kinase signaling. *Plant Signal Behav* 6:8–12.
62. Qiu JL, et al. (2008) Arabidopsis mitogen-activated protein kinase kinases MKK1 and MKK2 have overlapping functions in defense signaling mediated by MEKK1, MPK4, and MKS1. *Plant Physiol* 148:212–222.
63. Kong Q, et al. (2012) The MEKK1-MKK1/MKK2-MPK4 kinase cascade negatively regulates immunity mediated by a mitogen-activated protein kinase kinase kinase in Arabidopsis. *Plant Cell* 24:2225–2236.
64. Brader G, Djamei A, Teige M, Palva ET, Hirt H (2007) The MAP kinase kinase MKK2 affects disease resistance in Arabidopsis. *Mol Plant Microbe Interact* 20: 589–596.
65. Teige M, et al. (2004) The MKK2 pathway mediates cold and salt stress signaling in Arabidopsis. *Mol Cell* 15:141–152.
66. Matsuoka D, et al. (2002) Activation of AtMEK1, an Arabidopsis mitogen-activated protein kinase kinase, in vitro and in vivo: Analysis of active mutants expressed in E. coli and generation of the active form in stress response in seedlings. *Plant J* 29: 637–647.
67. Dubois M, et al. (2015) The ETHYLENE RESPONSE FACTORs ERF6 and ERF11 antagonistically regulate mannitol-induced growth inhibition in Arabidopsis. *Plant Physiol* 169:166–179.
68. Zhai Q, et al. (2015) Transcriptional mechanism of jasmonate receptor COI1-mediated delay of flowering time in Arabidopsis. *Plant Cell* 27:2814–2828.
69. Zhou X, et al. (2016) The ERF11 transcription factor promotes internode elongation by activating gibberellin biosynthesis and signaling. *Plant Physiol* 171:2760–2770.
70. Zhu L, Liu D, Li Y, Li N (2013) Functional phosphoproteomic analysis reveals that a serine-62-phosphorylated isoform of ethylene response factor110 is involved in Arabidopsis bolting. *Plant Physiol* 161:904–917.
71. Shyu C (2016) Unwinding JAZ7–Enigma to harmony. *J Exp Bot* 67:3183–3185.